Silicon based high performance Anode Materials for Next Generation Li-Ion Batteries

Christian Pöpsel[1]
Prof. Graeme Blake[1]*

Abstract

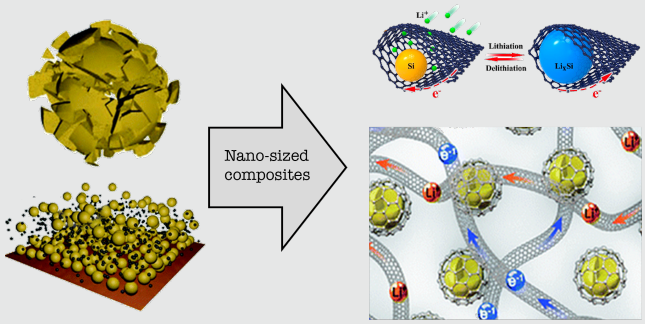

Anodes based on silicon are one of the most promising candidates for the next generation high performance Li-ion batteries, due to Si's high theoretical lithium storage capacity of 4200 mAh g^{-1}, which is more than ten times that of currently used graphite based materials. However, upon lithiation, Si exhibits a volume expansion of more than 400%, which leads to severe problems regarding stability and capacity retention, that need to be addressed in order to implement these anodes into real batteries. In this work, several promising recent designs, based on nano-sized structures in the range from 0D to 3D, are presented and critically reviewed. While materials mainly consisting of Si exhibit very high capacities, the electrochemically best performing designs tend to be hierarchical compounds. Especially promising are Si/C compounds of low dimensions that form 3D arrays. Often, the active material is integrated into a carbon based network, which provides high electronic conductivity, short Li-ion diffusion pathways and a rigid matrix that can ease the mechanical stress caused by the strong volume change upon lithiation and delithiation. Thus such designs exhibit a high retention of their capacity during many charge/dis-charge cycles as well as at high current densities. Apart from a high capacity and stability during cycling, some important parameters still need to be optimised in order to achieve commercialisation, such as increasing the coulombic efficiency and the areal mass load, as well as simple and cost effective synthesis methods. Despite these remaining issues, Si based anodes are about to emerge from the laboratories into real applications.

[1] *Zernike Institute for Advanced Materials, University of Groningen, Nijenborgh 4, 9747AG Groningen, The Netherlands*
* Supervisor

Contents

Introduction

In the light of climate change and fading fossil fuel resources, powering our more and more energy demanding world is one of the great challenges of today's society. Sustainable, renewable energy sources are intensively studied in order to replace the traditional fossil fuel power sources. Since, however, most of those alternative energy sources rely on either wind, tides, the sun, etc., compared to the steady energy output of most traditional power plants, it remains a great challenge to store the energy until it is used.[1]

Among the available rechargeable electrochemical energy storage solutions, Lithium Ion-Batteries (LIB) are one of the most promising ones, since they are safe, provide a stable cycle life, and relatively high energy density. Thus LIBs are already implemented in most portable devices such as laptops and smartphones. For their widespread application, especially in electronic vehicles, the capacities and energy densities of current cells are, however, too small.[2] In order to improve their performance, intensive research has focused in the last years on improving the three main parts of LIBs: electrolyte, cathode and anode. For the latter one, silicon-based materials

have shown a huge potential, mainly due to the fact that Si has a more than ten times higher theoretical gravimetric capacity (4200mAh g^{-1}) [3] than the currently used graphite based electrodes.

Usually, anode materials for Li-ion based electrochemical storage are categorised in terms of the mechanism upon which the lithium is stored in the material, which are intercalation, conversion and alloying (Fig. 1)

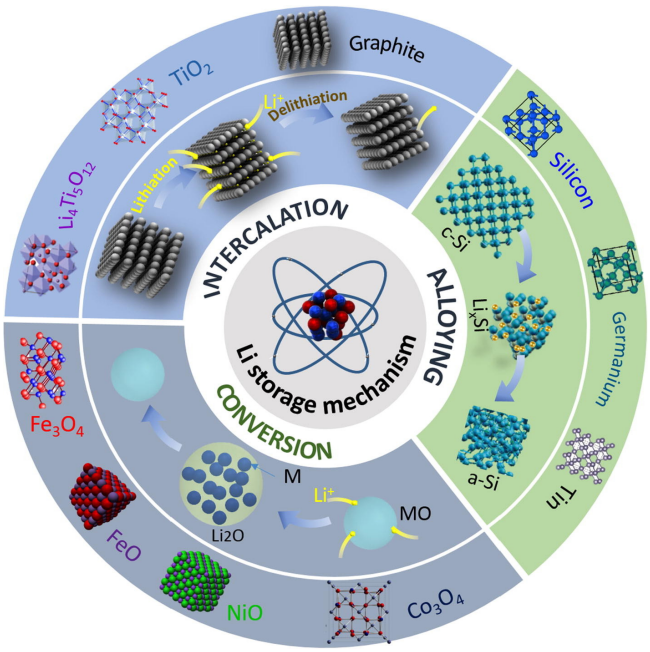

Figure 1. Different Li storage mechanisms of anode materials. From [4]

Intercalation/de-intercalation refers to the reversible insertion and extraction of lithium into a solid host network, which can have different crystal structures such as layered, spinel, olivine or favorite. The intercalation process does usually not result in a huge change in volume, which makes those materials very stable upon many charge/discharge cycles and is, amongst others, one of the reasons why since more than 20 years, commercially available Li-ion batteries rely on either layered graphite, or more recently also spinel $Li_4Ti_5O_{12}$ as an anode. These materials additionally provide desirable properties such as low cost, abundant availability, low delithiation potential vs. Li, high electronic conductivity, and ion diffusivity. [5] However, intercalation processes are usually not very efficient in terms of guest ions compared to host ions. Graphite, for example, can store one Li-ion for every 6 C atoms, which results in a relatively poor (theoretical) gravimetric capacity of 372 mAh g^{-1}. [3]

Conversion materials store Li ions according to the following mechanism:

$$Li + M_aX_b \leftrightarrow aM + bLi_nX \tag{1}$$

Here, M is often a transition metal and X represents an anion, which is often oxygen in the case of anodes. This class of materials tends to have a lot of beneficial properties, in particular, they show a high capacity (e.g. MnO with 755mAh g^{-1}[6]), are low cost and environment-friendly. However, they also show significant drawbacks, mainly a low coulombic efficiency (CE), unstable solid electrolyte interface (SEI) as well as poor cycling stability. [7]

Alloying/de-alloying is the third process upon which Li storage can take place and happens according to the following general mechanism, where M corresponds to either Si, Ge, Sn or Pb:

$$M + yLi \leftrightarrow Li_yM \tag{2}$$

Storing Li in materials by alloying shows very high (theoretical) capacities (Si: 4200 mAh g^{-1} [3]), as well as high energy densities and safe operations, but they show severe problems when it comes to cycling stability and capacity retention. Nevertheless, Si is subject to extensive research mainly due to its high storage potential and the fact, that Si manufacturing methods are highly developed due to its extensive use in the semiconductor industry. [7] Si additionally shows some beneficial intrinsic properties, such as a low delithiation potential vs. Li/Li^+ (0.4V) compared to most other anode materials, which results in a high working voltage and energy density. [8] On the other hand, the potential is higher than that of graphite (0.05V vs. Li/Li^+), and thus Si is less likely to form Li dendrites at high current densities. Those dendrites can lead to short circuits and ignition or explosions. [9]

A closer look into the alloying of Si provides a good basis to understand the origin of the extraordinary capacity, as well as the challenges that need to be addressed when using Si as an anode material. Typically, alloys are formed, such as Li_2Si, $Li_{21}Si_8$, $Li_{15}Si_4$, $Li_{22}Si_5$, which means, that up to 4.4 Li atoms per Si atom can be stored, compared to one Li atom per six C atoms in graphite. Silicon can either be amorphous (a-Si), poly-crystalline (p-Si) or crystalline (c-Si), with the latter one showing the highest electronic conductivity of the three. It has been found, however, that c-Si undergoes a phase transition upon the first lithiation, changing from a crystalline to an amorphous state, and remains amorphous during further cycling. It should be noted, that the final Li-Si alloy might be a metastable crystalline state.[11][12] Recently, a combination of focused ion beam time-of-flight secondary-ion-mass-spectrometry and auger electron spectroscopy were used by Bordes et. al. to investigate Si particles during the first lithiation process. The first 5% of Li form a solid-electrolyte interface (SEI), followed by a two-phase lithiation, characterized by a sharp edge between the alloy shell and the pure Si core. Fast diffusion pathways for the Li have been found that penetrate the pure Si core due to subgrain boundary pathways (Fig. 2). After 70% lithiation, the core-shell structure disappears and the particle starts to show damage.[10] Figure

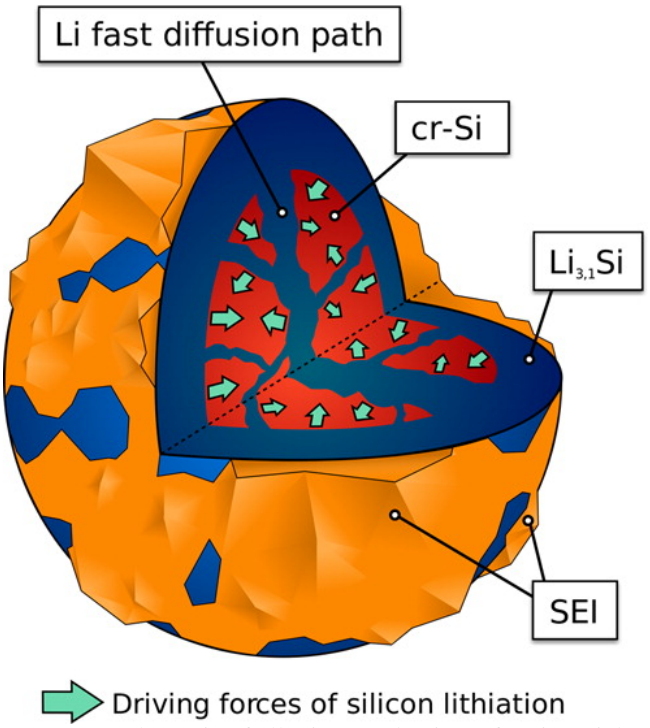

Figure 2. Schematic of alloying mechanism of a Si particle during first lithiation. A two phase mechanism with a sharp boarder between core (pure Si) and shell (alloy) and Li diffusion pathways penetrating the core has been observed. From [10]

3 shows TEM images of a Si nanoparticle (NP) during the first lithiation, clearly revealing the boundary between the lithiated and the pure Si phase. These studies further showed, that upon the first lithiation, c-Si particles show an anisotropic lithiation with facet formation. After full lithiation, the c-Si stays amorphous and further cycling occurs in an isotropic, single phase mechanism (Fig. 3).[13]

The capability of Si to store vast amounts of Li is accompanied by the side effect of huge volumetric changes of up to 420% during lithiation/de-lithiation.[14] This results in strong capacity fading and cell failure, mainly due to the following three effects (Fig. 4) :

Pulverization and cracking of the anode material occurs due to stress induced by the volume change upon lithiation/de-lithiation. This leads to loss of electric contact of the active material with the conducting framework or the current collector and thus capacity fading upon cycling.[15][16]

Delamination and morphology change are a result of structural change upon cycling. During lithiation, the Si particles or structures expand and impinge on each other, whereas during delithiation they contract, which can cause loss of conductive contact. Additionally, also on a bigger scale, the whole electrode expands and contracts, which can further cause cell failure.[14]

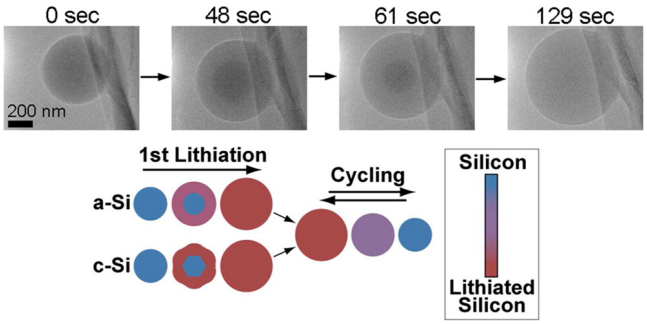

Figure 3. TEM images of a Si nanoparticle during the first lithiation, showing a two phase mechanism. The schematic shows the isotropic lithiation of a-Si compared with the anisotropic lithiation with facet formation of c-Si during the first cycle. After full lithiation, c-Si remains in an amorphous state. During further cycling, the lithiation is isotropic and a one-phase mechanism. From[11]

Unstable Solid-Electrolyte-Interface (SEI) formation can be attributed to irreversible Li-ion consumption due to their reduction on the electrode surface and thus the buildup of SEI. This layer is conductive for Li and covers the active material, which prevents further SEI build up and usually results in a smooth and thin SEI layer.[17] However, due to the large expansion of Si during lithiation, the SEI cracks open and exposes fresh Si. Subsequently, further electrolyte gets consumed and an inhomogeneous SEI with high resistance is formed. However, a thin, smooth and stable SEI is crucial to obtain little loss in capacity during cycling.[18]

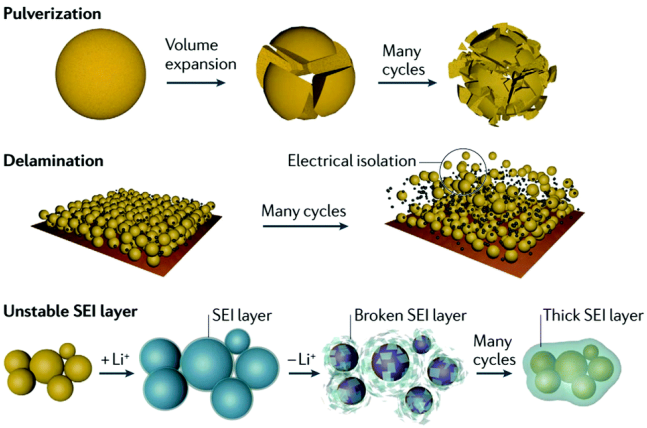

Figure 4. The three main effects that contribute to capacity fading and cell failure are depicted in a schematic way. They are all mainly caused by the drastic volume change of Si during lithiation and de-lithiation. From [11]

In order to address these issues and enhance the performance of anodes, various different strategies and approaches exist. Figure 5 shows an overview of the most common ones. The main goals are to compensate or accommodate the huge volume change of Si during cycling, facilitate electrochemical reactions by providing fast and short lithium ion diffusion

pathways, a high surface to volume ration as well as good electronic connectivity with the current collector and finally to ensure a smooth, thin and stable SEI formation.[11]

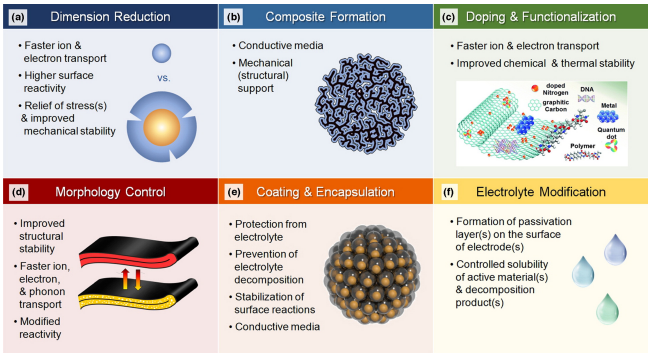

Figure 5. Overview of different approaches to enhance anode performance and counteract the problems associated with Si as an anode material. Most of them incorporate in one way or another the field of "nanoscience". From [5]

Nanotechnology and structural design have proven to be one of the key technologies to enhance anode performance, with a couple of structural designs ranging from 0D to 3D, which are found to be the bases of most structures (Fig. 6). In the light of the vast amount of research and thus different designs for Si-based anodes, it is helpful to summarise a few general properties and issues that are common for structures of a certain dimensionality, regardless of the specific materials used.

0D nanoparticles with diameters smaller than 150nm can expand upon first cycling without showing any damage, whereas diameters over 150nm exhibited severe cracking.[19] Although only the first lithiation was studied, these results do show the huge potential of 0D nanoparticles Si (NPs) to accommodate the huge volume change, if they are small enough. Anodes based on pure Si NPs do, however, suffer from electrochemical aggregation, since they tend to accumulate upon many cycles of expansion and contraction and disconnect from the current collector. They also exhibit a large surface area, leading to unwanted side reactions and extensive SEI formation. Often, these effects are counteracted by implementing the NPs into a stabilising and/or conducting matrix or grid.[11][20]

1D nanorods, nanowires and nanotubes provide a good conductivity due to the 1D transport channel along them, and the fact, that they are usually directly grown onto the current collector.[20] They tend to fracture less than 0D NPs upon lithiation because the volume change associated with that is usually anisotropic and the radial expansion induces less stress that can lead to cracking. Furthermore, the space between the nanorods can accommodate the volumetric change, all of which leads to a high cycling stability as well as a high reversible capacity.[22] Nanotubes additionally provide accessible channels for electrolyte transport and short lithium ion diffusion pathways, as well as internal space for volume expansion. On the other hand, the high specific surface of

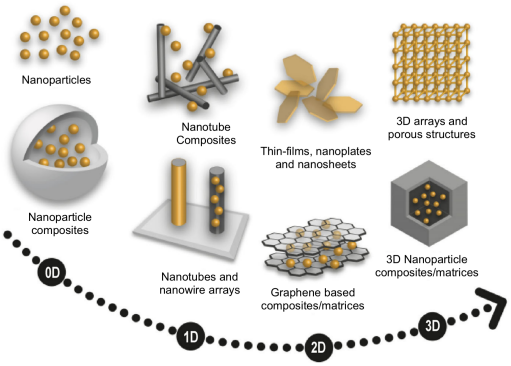

Figure 6. Most common nano-structures found in novel anode designs. Adapted from [21]

1D structures leads to more irreversible reactions and thus to a higher SEI build up.[20] [11] A common approach are double wall nanotubes, where a rigid outside coating prevents outward expansion which promotes the formation of a stable SEI layer, while Li ions can still diffuse through this capping. [23]

2D thin films and nanoplates show generally a high capacity retention upon cycling, but they tend to crack upon the first lithiation and thus show strong capacity fading during the first cycles. For thin films it has been found, that decreasing their thickness increases the reversible capacity and cycling stability.[11] Si nanosheets exhibit very short lithium diffusion pathways, little volume expansion and are highly compatible with other materials.[20] 2D materials, especially graphene, are also used as a matrix for 0D NPs. As mentioned earlier, pure SiNP anodes suffer from aggregation and electrode destruction due to volume change and low electronic conduction. Implementing NPs in matrices buffers the huge volumetric expansion of Si and enhances the electronic conductivity, since graphene is highly conductive.[24]

3D Si-based porous structures and networks can accommodate the volumetric changes due to their porous character and thus maintain structural integrity while having a much higher tap density, and thus theoretically a much higher volumetric capacity, than nanostructures of lower dimensionality. The tap density measures the density of a powder after tapping the container that contains the material. 3D structures also provide fast lithium diffusion through their pores, but similar to 0D and 1D approaches, composites usually show better performance than pure Si structures. [11][20]

Recent novel designs for Si based anodes

In the following, a couple of promising and well-performing approaches out of the vast amount of work done in the field are reviewed and looked at in more detail. The presented anodes are either performing very well, show a high stability, feature

an interesting design or stand out for some other reason.

0D structures

Pure Si nanoparticles (SiNPs): Lin et al. prepared Si nanocrystals with a size ranging from several tens to 100nm from $SiCl_4$ in the molten salt of $AlCl_3$. During the first cycling, a plateau at 0.1V vs. Li/Li^+in the discharge curve was observed (Fig. 7a), which corresponds to the Li-Si alloying reaction. Note, that charge-discharge curves are a valuable tool to investigate the electrochemical processes during the first couple of lithiation/de-lithiation cycles due to their distinctive plateaus and shapes. However, discussion of these curves for each of the materials reviewed in this work would go too far into detail. Figure 7b shows a SEM image of the material, which exhibits a high initial coulombic efficiency (ICE) of 84.7% and a high reversible capacity of 1180mAh g^{-1} after 500 cycles at a current density of 3000mA g^{-1} with a coulombic efficiency (CE) over 98% (Fig. 7c). The good stability is mostly attributed to the capability of the SiNPs to expand and contract during cycling without cracking.[25]

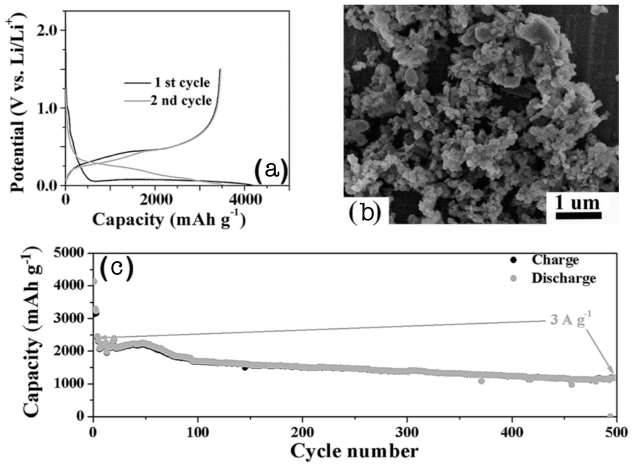

Figure 7. a) Charge/discharge curve of first cycle with plateau at 0.1V corresponding to Li-Si alloying. b) SEM image of SiNPs. c) SiNPs show high capacity retention of 1180mAh g^{-1} after 500 cycles at a high current density of 3000mA g^{-1}. Adapted from [25]

Yolk-Shell structure Si@C@void@C: These nanohybrids consist of a Si core (50-100nm), an inner carbon shell (10nm), a 50nm void space and a 10nm outer C shell, which are synthesised as shown in figure 8B,E. Similar to traditional Si@void@C yolk-shell structures (Fig. 8A), they greatly improve the ionic and electronic conductivity compared to pure SiNPs or Si@C core-shell structures. The void space accommodates the volume change upon charge and discharge, and the additionally introduced inner C shell in this novel design increases the conductivity between the Si and the hollow C shell as well as effectively protects the Si from direct contact with the electrolyte and thus strong SEI formation. Compared to related structures, the Si@C@void@C anode shows an enhanced reversible capacity of 1366mAh g^{-1} after 50 cycles at 500mA g^{-1} (Fig. 8C) as well as a good rate performance with 60% capacity retention at 4000mA g^{-1}.[26]

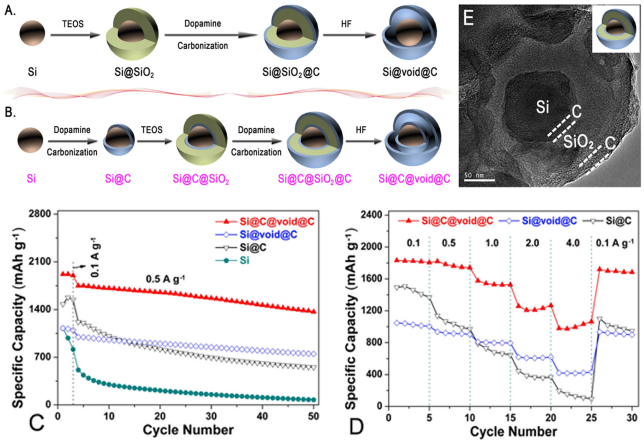

Figure 8. A,B) synthesis of traditional yolk-shell and Si@C@void@C structures (TEOS = tetraethoxysilane). C) the novel material shows superior cycling stability (1366mAh g^{-1} after 50 cycles at 500mA g^{-1}) than related structures and D) also enhanced rate performance (1009mAh g^{-1} at 4000mA g^{-1}). E) shows a TEM image of a precursor of the Si@C@void@C structure before HF etching. Adapted from [26]

Non-filling carbon-coated porous Si micrometer particles (nC-pSiMPs): To avoid the problems of fracturing and SEI instability, silicon micrometer particle (SiMP) structures have been synthesised by Lu et al. They heated resin coated SiO microparticles, which lead to a phase separation and thus to interconnected Si-NPs (<10nm) embedded in a SiO_2 matrix as well as a transformation of the resin to a C layer. Finally, HF was used to etch the SiO_2, which leaves void spaces that allow the Si to expand during lithiation without damaging the carbon coating. For comparison, impregnation coated porous Si microparticles (iC-pSiMPs) and non-coated pSiMPs have been synthesised as well. During the first cycling, the impregnation coating breaks and exposes the Si to the electrolyte, resulting in a thick, non-uniform formation of SEI (Fig. 9a top), whereas the nC-pSiMPs have enough space to expand without rapturing the external carbon coating, which leads to a uniform and thin SEI (Fig. 9a bottom). Figure 9b shows TEM images of a C-pSiMP at the beginning and after 150 seconds of lithiation. It can be seen that clearly, the structure remains intact, while the SiNPs in the inside expand without fracturing the outer C coating. This behaviour is the main reason for the superior cycling stability with 1490mAh g^{-1} retained capacity after 1000 cycles at 1050mA g^{-1}.[27]

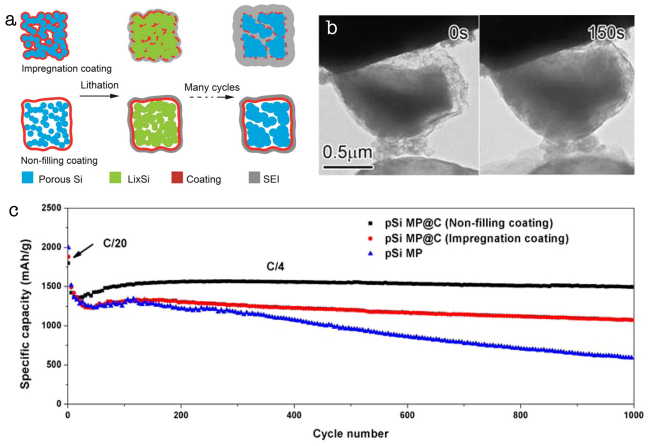

Figure 9. a) Rupture of impregnation C coating upon lithiation leading to a thick SEI vs. thin and smooth SEI formation around the non-filling coated microparticles. b) shows TEM images of a nC-pSiMP at the beginning and after 150s of lithiation, clearly exhibiting internal volume expansion of the Si nanoparticles without damaging the external C coating. c) Superior cycling stability of nC-pSiMPs with 1490mAh g^{-1} retained capacity after 1000 cycles at 1050mA g^{-1}. Adapted from [27]

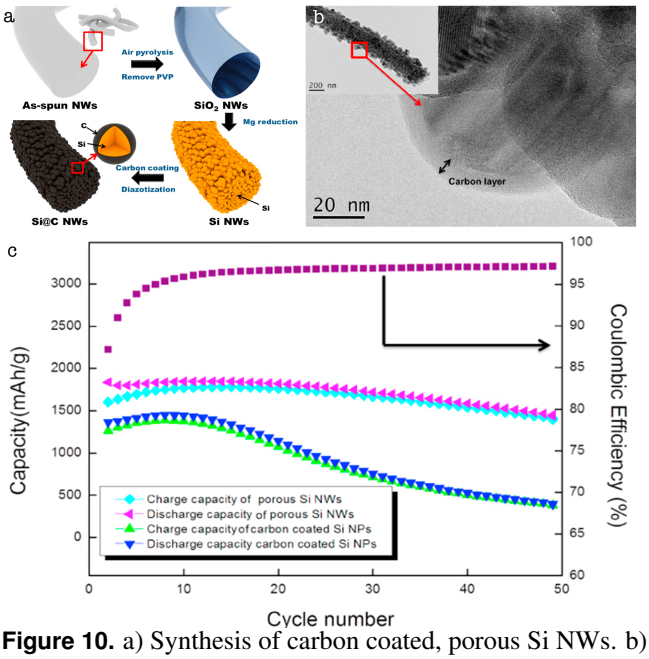

Figure 10. a) Synthesis of carbon coated, porous Si NWs. b) TEM images showing the porous, crystalline nature of the Si NWs (inset) as well as the carbon coating. c) Cycling stability of C coated Si NWs vs. similarly processed Si NPs. The NWs outperform the 0D structured anode, showing 1500mAh g^{-1} after 50 cycles at 400mA g^{-1}. Adapted from [28]

1D structures

Porous, carbon coated Si Nanowires: By electrospinning a polymer blend (PVP), followed by an Mg reduction, highly porous NWs of interconnected, 50nm sized Si nanocrystals were fabricated by Yoo et al. Finally, a multilayer carbon coating was applied, which uniformly covers the inner and outer parts of the NWs (Fig. 10a,b). This structure exhibits a large capacity loss during the first cycles, which is most likely attributed to residual SiO_2, which could not be removed, and irreversibly takes up Li during the first discharge. However, compared to carbon-coated Si nanoparticles anodes synthesised by a similar process, the NWs show superior cycling performance and a capacity of 1500mAh g^{-1} was retained after 50 cycles at 400mA g^{-1} (Fig.10c). This enhanced performance is attributed mainly to the interconnected and porous nature of the NWs. While the pores accommodate the volume change, the interconnection and the carbon coating enhance Li-ion and electron conductivity. TEM investigations after 100 cycles showed that while NWs with diameters below 300nm remained complete, bigger diameters lead to deformation and fracture, which partly explains the reduction of capacity with continuous cycling.[28] This observation is in very good agreement with other reports, that also state a critical diameter of 300nm for Si NWs, below which the elastic stress released upon lithiation is small enough to not cause damage. Thus precise control over the NW diameter is crucial for good cycling stability.[29]

C@Si@C Core-Shell hollow Si Nanotubes (h-SiNT): These hollow, double carbon-coated Si nanotubes are fabricated by depositing Si on an MgO template via low-pressure CVD, followed by an etching step to remove the template and finally a 50nm carbon coating inside and outside the hollow Si tube (Fig.11a). After 120 cycles at 1000mA g^{-1}, 975mAh g^{-1} remained and upon further cycling at 3000mA g^{-1}, 700mAh g^{-1} capacity was retained after 300 cycles, which corresponds to a loss of only 0.022% per cycle. Although the carbon coating reduces the theoretical capacity of the anode, it provides mechanical reinforcement and enhanced surface conductivity, and as a result, stablises cycling. The anode additionally exhibits excellent rate capability and retention, with a capacity of 1250mAh g^{-1} retained at 1000mA g^{-1} after current densities up to 5000mA g^{-1} have been applied (Fig. 11c). [30]

0D Si nanoparticles encapsulated in TiO_2 nanotubes: The fabrication process of this combined 0D and 1D design consists of three basic steps. First, the TiO_2 nanotubes are directly grown on a titanium base, which also acts as a current collector. That way, the hollow tubes not only provide a supporting structure for the active material, but they also act as a highly conducting framework, since the tubes are directly connected with the current collector without any intermediate binder. Second, the Si nanopowder was inserted into the NTs by a simple brushing technique. Finally, a binder layer was used to seal the tubes. To confirm the successful preparation of the structure (Fig.12a), especially a sufficient insertion of the Si nanopowder, SEM and EDS imaging was used (Fig.12b). This data clearly shows several hundreds of nanometers of

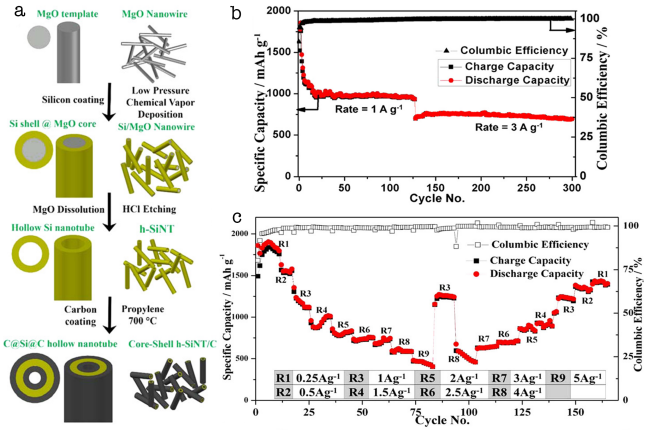

Figure 11. a) Synthesis steps to obtain a C@Si@C core-shell hollow nanotube structure. b) Excellent cycling stability with only 0.022% capacity loss per cycle leading to a remaining 700mAh g^{-1} after 300 cycles at 3000mA g^{-1}. c) High retention of capacity, even after high current densities were applied to the anode. Adapted from [30]

inserted Si powder by the simple brushing approach. Electrochemical performance measurements showed a high capacity of 1824.9mAh g^{-1} after 300 cycles at 420mA g^{-1} current density (Fig.12c). However, even after 300 cycles, a considerable loss was observed in each cycle, which suggests, that some irreversible Li consumption takes still place after many cycles and thus, there is still room for improvement.[31]

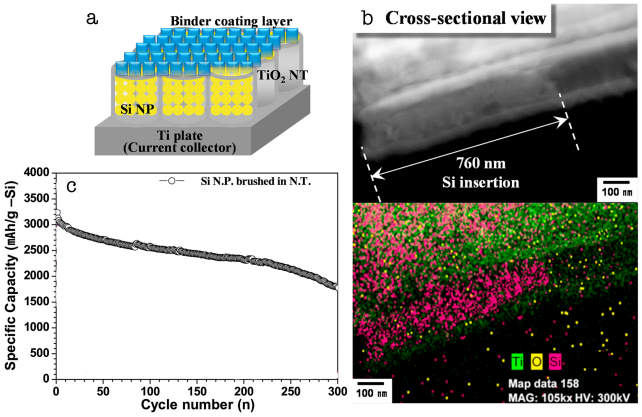

Figure 12. a) schematic of the intended structural design by brushing Si nanopowder into TiO_2 nanotubes. b) SEM and EDS data confirms a good degree of filling of the NTs. c) high capacity of 1824.9mAh g^{-1} after 300 cycles at 420mA g^{-1} maintained, but no saturation even after 300 cycles. Adapted from [31]

Bio-inspired sandwich structured C@Si@TiO_x nanofiber composite: The starting material for these bio-inspired structures is a filter paper, on which a thin silica and an even thinner titania film were deposited, leading to a cellulose/silica/titania nanofiber structure as a precursor. After carbonization of the cellulose core and Mg assisted reduction of the silica and titania, finally the desired C/Si/TiO_x nanofiber structure was obtained (Fig.13a) and confirmed by TEM imaging (Fig.13b). The diameters of the entire fibers range from 100nm to 300nm, while the Si layer has a thickness of about 50nm and the TiO_x layer of about 5-10nm. The individual nanofibers then form a 3D network-like, hierarchical structure, which exhibits very good electrochemical performance, especially compared to similar fibers, that consist of only parts of the whole C@Si@TiO_x layers. Although the initial CE is relatively low at 53.4%, which is mostly due to formation of an SEI layer and the irreversible reduction of electrolyte upon the first cycles, the reversible capacity is good with 792.6mAh g^{-1} after 160 cycles at 100mA g^{-1} (Fig.13c) and a good rate capability was obtained, where 176.2mAh g^{-1} where maintained at 3000mA g^{-1} current density(Fig.13d). The superior electrochemical performance of the entire structure compared to nanofibers with fewer layers, is attributed to the beneficial combination of a carbon scaffold and TiO_x coating, both of which enhance ionic and electronic conductivity. At the same time, these layers stabilize the structure during lithiation/de-lithiation and buffer the volume change, which helps to maintain the structural integrity.[32]

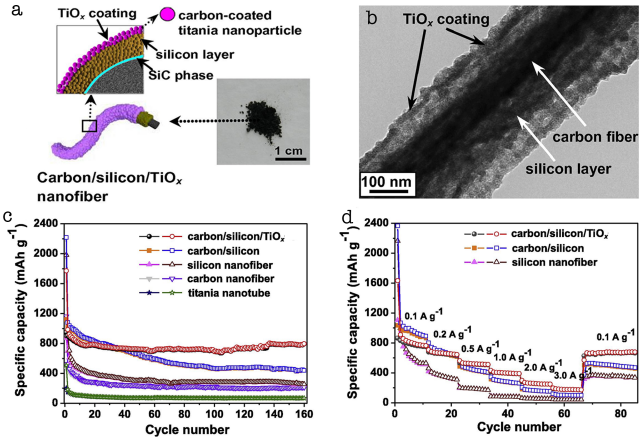

Figure 13. a) Schematic structure of C@Si@TiO_x nanofiber; the inset shows a photograph of the composite. b) TEM image of a nanowire showing the C core and the Si and TiO_x layer. c) Enhanced cycling stability of entire structure exhibiting 792.6mAh g^{-1} after 160 cycles at 100mA g^{-1}. c) Superior rate capability of entire structure, which maintains 176.2mAh g^{-1} at 3000mA g^{-1}. Adapted from [32]

Branched NW Ge/Si heterostructures: Kennedy et al. grew wormlike germanium nanowires directly on a stainless steel current collector, which ensures efficient 1D electron transport along the Ge NW and also high conductivity between the NW and the collector since no additional binder needs to be used. With SN nanoparticles as seeds, Si nanowires are then grown along the Ge structures (Fig.14a). SEM images show how the Si NWs wrap around the Ge NWs, creating a core-shell like structure, with the important difference, that unlike a typical core-shell structure, the Si is not constrained

by the Ge. This results in less mechanical strain induced into the material upon charge/dis-charge since both materials can expand and contract independently, which enhances the cycling life and rate capability. The average diameter of the Ge and the Si NWs have been found to be 74nm and 14nm, respectively (Fig.14b). Three different Ge:Si ratios have been fabricated and compared in terms of their electrochemical performance. Generally, the more Si-rich the structure is, the higher its capacity, while more Ge rich wires exhibit a better capacity retention as well as a higher rate capacity (Fig.14c,d). This makes it possible to tailor the electrochemical characteristics of this composite towards different needs by simply changing the Ge:Si ratio. The most stable structure was found to be the 4:1 (Ge:Si) type, which shows a stable reversible capacity of 1256mAh g^{-1} after 100 cycles at 840mA g^{-1}, as well as an incredible rate performance of 802mAh g^{-1}, even at such high current densities as 42000mA g^{-1}. Figure 14d also shows clearly, that with increasing rates, the Ge:Si heterostructures quickly outperform pure Si nanowires, regardless of their specific Ge:Si ratios. Kennedy et al. also observed, that the branched NW structures transformed into a Ge-Si alloyed network upon cycling.[33]

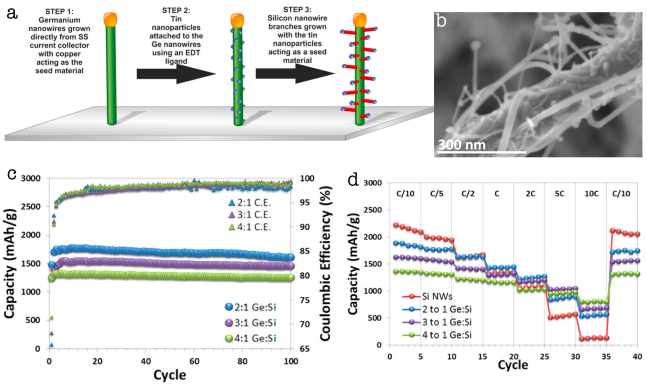

Figure 14. a) Synthesis steps for Si/Ge branched nanowires on a stainless steel (SS) current collector. b) SEM image showing how the Si branches wrap around the Ge NW, forming a core-shell like structure. c) Si rich structures exhibit higher capacities, while the capacity retention on cycling is more stable for a lower Si content. (4:1-Ge:Si retain 1256mAh g^{-1} after 100 cycles at 840mA g^{-1}). d) Ge rich heterostructures show a better rate capability, up to very high current densities (4:1-Ge:Si has still 802mAh g^{-1} at 42000mA g^{-1}) Note, that in this graph, 1C equals a current density of 4200mA g^{-1}. Adapted from [33]

2D structures

Mesoporous Silicon nanosheets wrapped in Carbon: A mesoporous silica precursor is reduced, using magnesium at high temperatures, which results in 2D nanosheets of mesoporous Si with an average pore diameter of 5.65nm (Fig.15a). Subsequently, a carbon coating between 5nm and 15nm is applied via a self-assembly process and thermal polymerization. In comparison with non-coated Si nanosheets and pure Si nanoparticles, the carbon wrapped structure shows less irreversible capacity loss during the first cycle as well as a superior cycling stability (Fig.15c). The carbon wrapped sheets not only outperform the other structures at high current densities (1296.6mAh g^{-1} at 4000mA g^{-1}) (Fig.15d) , but even at such high rates, they maintain a capacity of 1072.2mAh g^{-1} after 500 cycles. This corresponds to a coulombic efficiency of ≈100% (Fig.15b). This impressive stability is likely attributed to the interplay of the thin 2D structure, that shortens the Li diffusion pathways and buffers the structural stress upon volume change, the carbon layer, which improves electronic conductivity, as well as the porous structure, which buffers the volume expansion and accelerates the electrolyte permeation. TEM images of the carbon-coated structure and a pure mesoporous Si structure after 100 cycles show severe cracking and pulverization for the former (Fig.15e), while the latter maintained its structure, apart from the formation of a smooth and uniform SEI layer (Fig.15f).[34]

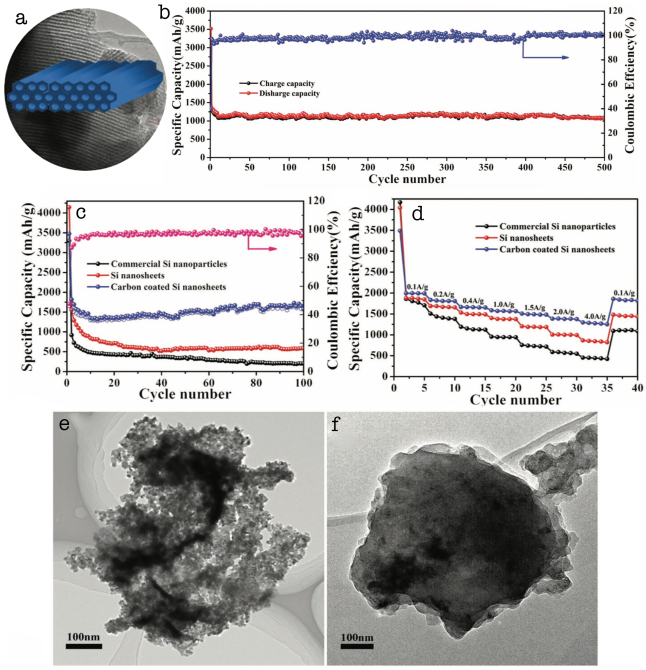

Figure 15. a) Mesoporous Si nanosheet structure in front of its TEM image, which was used to measure the pore size. b) The structure shows very high cycling stability and a CE of ≈100% even at high current densities (1072.2mAh g^{-1} after 500 cycles at 4000mA g^{-1}). c) Carbon coated structure shows superior stability compared to non-coated Si nanosheets and commercial Si NPs, as well as d) A superior rate capability with 1296.6mAh g^{-1} at 4000mA g^{-1}. e) TEM image of non C-coated Si sheet after 100 cycles shows severe cracking and pulverization. f) C coated sheet after 100 cycles shows no damage and a smooth SEI layer. Adapted from [34]

Si nanoparticles wrapped in 2D carbon nanosheets: The wrapping of 50nm Si nanoparticles into 2D carbon nanosheets was done via a one-pot salt synthesis and thermal carbonisa-

tion of glucose (SEM image Fig.16b). Three different samples with different carbon contents were fabricated, where Si/C-0.3 corresponds to the lowest C content and Si/C-0.2 to the highest. Additionally, one sample of pure 2D carbon sheets and one of pure Si nanoparticles were synthesised for comparison. While the pure Si NP anode suffers from huge capacity loss after a few cycles, the pure carbon sample maintains a stable, but very small capacity. The Si/C structure, on the other hand, provides high capacities with stable cycling, with the intermediate Si/C-0.25 sample showing the best capacity retention of 881mAh g^{-1} after 500 cycles at 420mA g^{-1} (Fig.16d). This specific sample also shows a good rate capability with 401mAh g^{-1} at 3100mA g^{-1} (Fig.16c). The main reason for the good electrochemical performance lies in the carbon wrapping, which provides not just a highly conductive network with good contact, but also stabilises the Si NPs while they expand and contract during lithiation/de-lithiation (Fig.16a).

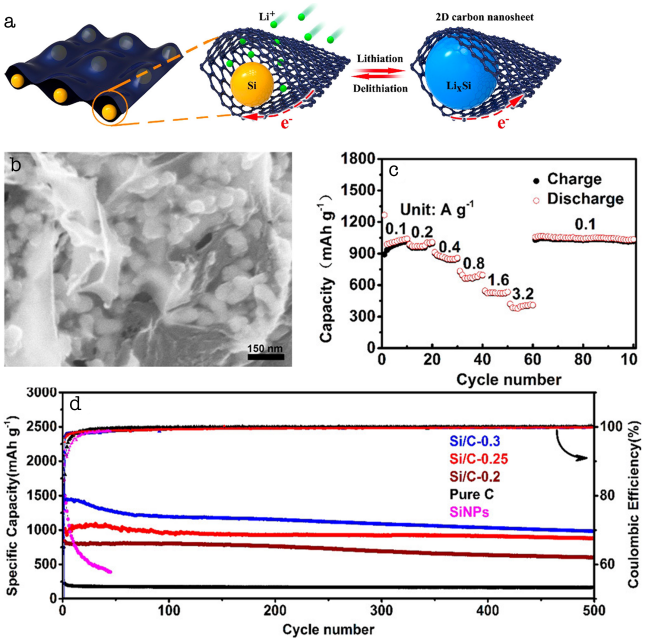

Figure 16. a) The 2D carbon sheets stabilize the Si NPs during charge/dis-charge and provide a conductive network. b) SEM image of the carbon wrapped Si NPs. c) Good rate capability of the Si/C-0.25 sample with intermediate C content (401mAh g^{-1} at 3100mA g^{-1}). d) Comparison of the cycling stability of different, but similarly synthesised anode materials, where the sample with the intermediate C content (Si/C-0.25) shows the least capacity fading and retains 881mAh g^{-1} after 500 cycles at 420mA g^{-1}. Adapted from [35]

3D structures

Carbon wrapped porous silicon: Gao et al. prepared carbon wrapped and carbon-coated porous Si samples by reducing SiO bulk material, using magnesium at high temperatures, followed by selective HF and HCl etching steps, which results in a porous Si (PSi) bulk with pore sizes <50nm. These are then either carbon wrapped (CWPSi) (Fig.17a, top) or carbon coated (CCPSi), where the carbon coating infiltrates into the pores (Fig.17a, bottom). A TEM image of the CWPSi sample is shown in figure 17b. In terms of electrochemical performance, the carbon wrapping seems to be beneficial in terms of cycling stability as well as rate capability. The CWPSi achieved a capacity of 1639mAh g^{-1} after 200 cycles at 1000mA g^{-1} (Fig.17c), and retained 1074.1mAh g^{-1} even at 4000mA g^{-1} (Fig.17d). Compared to the infiltrating carbon coating, the wrapping allows the Si to expand and contract inside without cracking the outer layer, which leads to less, and smoother SEI formation. Thus, less volume change of the whole anode was observed during cycling for the CWPSi material.[36]

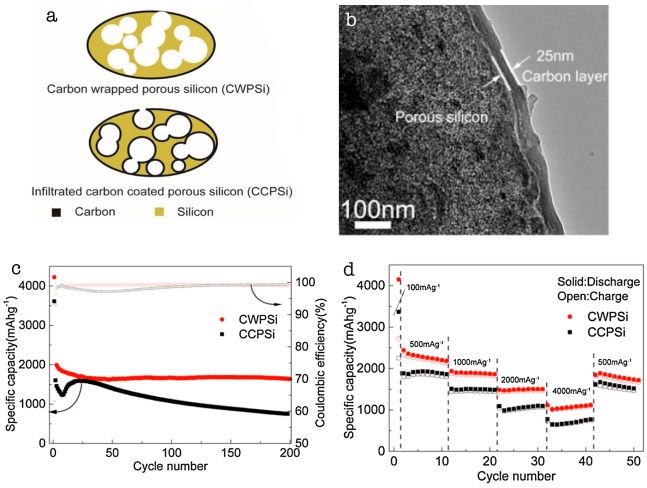

Figure 17. a) Schematic of the two compared structures, carbon wrapped and carbon coated. b) TEM image of the carbon wrapped material. c) The CWPSi shows a better cycling stability with 1639mAh g^{-1} retained after 200 cycles at 1000mA g^{-1}. d) The wrapping also improves performance at high rates, maintaining a capacity of 1074.1mAh g^{-1} at 4000mA g^{-1}. Adapted from [36]

Structure-preserved 3D porous Si/reduced graphene oxide (Si/rGO): Zhang et al. synthesised different silicon/reduced graphene oxide (Si/rGO) composites by changing the evaporation drying time of a solvothermally prepared Si/rGo hydrogel precursor, in which the Si nanoparticles are wrapped into the graphene sheets (Fig.18a). For drying times of 0h, 2.5h, and 3.5h, the pore size gradually decreased from 10μm to 500nm, while for 4h drying time no porous structure could be observed. The only sample, that remained its structural integrity during the grinding and compression processes necessary to produce an electrode, was the one with 500nm pore size after 3.5h of drying time. Figure 18b shows an SEM image of that sample. Featuring structural integrity, which ensures short Li migration pathways and superior electrolyte infiltration, as well as stable SEI formation in combination with an interconnected, conducting 3D framework, the electrochemical performance of Si/rGO-3.5 surpasses that of the

other samples. It shows a capacity of 955mAh g^{-1} at 2000mA g^{-1} current density (Fig.18c), and retains 1210mAh g^{-1} after 100 cycles at 500mA g^{-1} (Fig.18d). The sample without any pores (Si-G-4) performs significantly worse than the others, which indicates that those pores are crucial for a good electrochemical performance.[37]

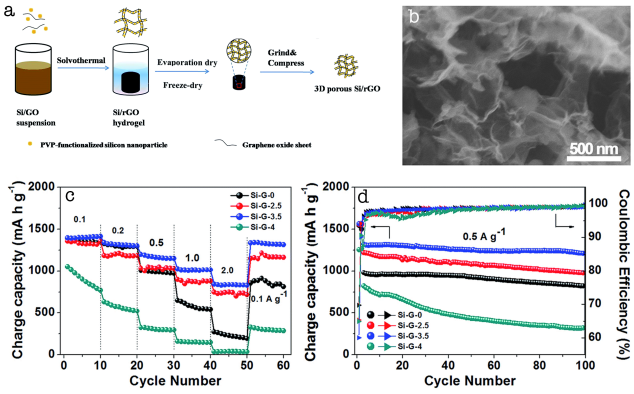

Figure 18. a) Synthesis steps of the silicon/reduced graphene oxide (Si/rGO) samples. b) SEM image of 500nm pore structure after 3.5h evaporation drying time. c) Si/rGO-3.5 samples shows highest rate capability with 955mAh g^{-1} at 2000mA g^{-1}. d) It also shows stable cycling and retains 1210mAh g^{-1} after 100 cycles at 500mA g^{-1}. Adapted from [37]

Graphene encapsulated Si nanoparticles in a carbon nanotube network: This highly hierarchical composite, consisting of 0D, 1D and 2D materials forming a 3D network (Si@Gra@CNT), is synthesised based on CVD using Cu as a catalyser for the graphene and carbon nanotube (CNT) growth (Fig.19a) The CNTs have an average length of 5μm and 10nm diameter, acting as conductive bridges. The Si NPs are of 30nm in diameter and wrapped into graphene in a Si@void@graphene sub-structure. In the TEM image of the Si@Gra@CNT structure (Fig.19b), the CNTs, the Si NPs, and the graphene sheets can clearly be observed. For comparison, in addition to the Si@Gra@CNT sample, one sample without the graphene wrapping (Si@CNT) and one without the CNTs (Si@Gra) were synthesised. The initial CE of the Si@CNT electrode is significantly smaller than that of the samples with graphene, which can be attributed to a thick and non-uniform SEI formation since the protective graphene wrapping is missing. Overall, the full Si@Gra@CNT anode shows an outstanding electrochemical performance, with a rate capability of 800mAh g^{-1} at 8000mA g^{-1} current density (Fig.19c) and a long preservation of its reversible capacity of 983mAh g^{-1} after 1200 cycles at a relatively high current density of 2000mA g^{-1}. This impressive performance is most likely attributed to the following features of the Si@Gra@CNT design: the flexible nature of the CNTs, combined with the void space between the Si NPs and their graphene cages, can accommodate the volume change of the Si upon charge/dis-charge and thus ease the mechanical stress and maintain the structural integrity. Additionally, the graphene acts as a protection layer, which prevents direct contact between the electrolyte and the Si, and thus helps to build a stable, smooth and thin SEI layer. Finally, the carbon matrix of graphene and CNTs is highly conductive and provides efficient channels for fast charge transfer, which improves the kinetics of electrochemical processes.[38]

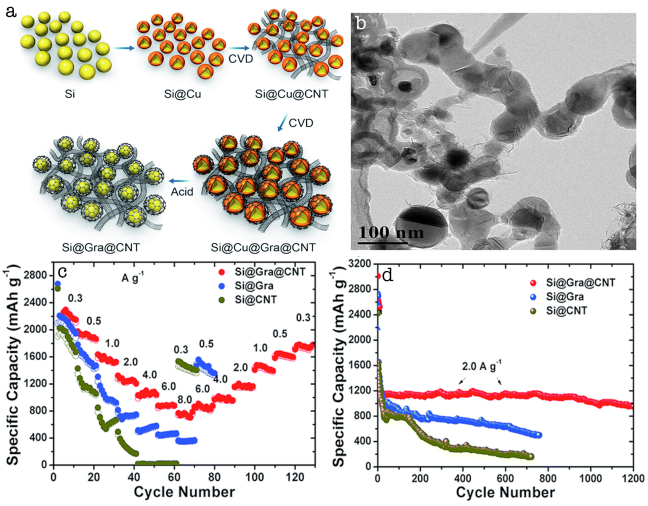

Figure 19. a) Schematic of synthesis of the Si@Gra@CNT composite. b) TEM image of the final sample, showing the CNTs, the Si NPs and the graphene wrapping. c) The full Si@Gra@CNT structure exhibits outstanding rate performance with 800mAh g^{-1} at 8000mA g^{-1}. d) Even after 1200 cycles at 2000mA g^{-1}, the full structure still preserves 983mAh g^{-1} of reversible capacity. Adapted from [38]

Conclusion and Outlook

Despite silicon being widely recognised as a promising anode material and a vast amount of researchers working on it, with partly impressive results in terms of electrochemical performance, there is still basically no implementation of Si-based anodes into commercial batteries, and one might wonder about the reasons.

Most of the materials found in publications are optimised towards high specific gravimetric capacities as well as high cycling stability and are usually tested in a half-cell setup. For the application in real batteries, however, there are a couple of other parameters, that might be equally or even more important.

As mentioned earlier, usually the materials are aimed to achieve a high specific gravimetric capacity, which often results in structures that exhibit very low tap densities. Low tap density, however, means that only little amounts of the material can actually be placed on the current collector, which directly influences the energy storage capacity of the full battery. Most works also show, if reported at all, a very low areal mass loading, which can be understood given the fact, that a low areal mass loading is beneficial in order to achieve

stable performance over many cycles. Unfortunately, a high areal mass loading is crucial for a decent energy output of real batteries, which is more and more recognised, but few studies have attempted to improve areal mass loading while maintaining a good capacity and cycling stability.[27]
Another parameter, that currently prevents the commercial use of most Si-based anodes is the coulombic efficiency. Most of the materials show initial CEs of 65% - 85%, which is very little compared to typical values of 90% - 94% for graphite-based anodes. And although a lot of Si-based structures exhibit CEs of 98% - 99.7%, which is enough to provide decent cycling stability in a half cell setup, these values must still rise to 99.9%. This is due to the fact, that in a full cell, a small change in CE can lead to severe capacity fading over a very small number of charge and discharge cycles.
Perhaps the main factor that determines whether a specific anode design actually makes it to the market is cost. This includes obviously raw materials costs, which is why silicon and silicon/carbon composites are of specific interest due to their high abundance. Furthermore, a tremendous amount of know-how for Si manufacturing already exists due to its intensive use in the semiconductor industry, which helps to keep costs low. However, since current research focuses mostly on the performance of Si-based anodes, often their synthesis is neither scalable to industry needs nor efficient or environment-friendly. Thus more focus on improving existing or inventing new synthesis methods for well-performing architectures will accelerate commercialisation and practical implementation of Si-based anodes.

Taking all the discussed parameters into account when comparing the figures of merit of the different structures and designs reviewed in this work (Table 1), one can observe, that the materials with the highest capacities are not necessarily those best suited to actual implementation in a real battery. There is also no obvious correlation between performance and a specific dimensionality, however, it seems as if the use of carbon, especially in the form of CNTs and graphene as a conductive and supportive matrix, tends to improve the cycling stability and coulombic efficiency. Also, composites and hierarchical structures seem to exhibit a very stable performance compared to mainly Si-based, more simple structured approaches. While structures of the latter category are often easier to synthesis, it still might be more fruitful to further explore the possibilities of Si/C based hierarchical composite structures as well as facilitate their synthesises. In fact, most recent papers actually tend to go down that road. It should be noted, that there won't be one anode that suits all needs and purposes, but rather different materials for either high capacities, ultra long lifetime or high energy output. This is also reflected in the summary of the materials reviewed in this work (Table 1), where each material shows specific weaknesses and strengths.

Finally, despite all the challenges and problems that still need to be overcome, silicon-based anodes are one of the most promising anode candidates for the next generation of Li-ion batteries and will likely drastically boost their performance compared to today's cells. Although there is still a long way to go until broad applications become feasible, recently the first reports on the commercialization of Si-based anodes have appeared. For instance, $3M^{TM}$ has a silicon-based anode powder on sale with twice the capacity of a standard graphite anode and a capacity retention of 70% after 500 cycles[39] and XG Science has a patent pending for a "silicon-graphene nano-composite anode material" with capacities between 600-2000 mAh g^{-1} and an initial CE of 85% [40].

Table 1. Figures of merit of reviewed structures

Material	Dimension	Initial CE	Initial charge capacity [mAh g^{-1}] @ current density [mA g^{-1}]	Initial discharge capacity [mAh g^{-1}] @ current density [mA g^{-1}]	CE	Reversible capacity [mAh g^{-1}] @ current density [mA g^{-1}]	Cycle number	Rate capabiliy capacity [mAh g^{-1}] @ current density [mA g^{-1}]	Areal Mass Loading [mg cm^{-2}]
Pure Si NPs [25]	0D	84.7%	4189	3549	>98%	1180 @ 3000	500	1180 @ 3000	N.A.
Yolk-shell structure Si@C@void@C[26]	0D	N.A	1910	N.A.	N.A.	1366 @ 500	50	1009 @ 4000	0.8
Non-filling Carbon coated porous Si micrometer-sized particles [27]	0D	78%	1798	N.A.	N.A.	1490 @ 1050	1000	N.A.	2.01
Porous Si NWs with C coating [28]	1D	N.A.	N.A.	3600	97%	1500 @ 400	50	N.A.	1
C@Si@C Core-Shell hollow Si Nanotube [30]	1D	88%	1565	1780	99.95%	700 @ 3000	300	600 @ 4000	1.7
0D Si particles encapsuled in TiO2 Nanotubes [31]	1D	76%	4262	3236	97.8%	1825 @ 420	300	N.A.	N.A.
Sandwich structured C/Si/TiO nanofiber composite [32]	1D	53.4%	946	1771	>98%	793 @ 100	160	176 @ 3000	1.6
Branched NW Ge/Si (4:1) heterostructures [33]	1D	71.4%	N.A.	1249	>98%	1256 @ 840	100	802 @ 42000	N.A.
2D Mesoporous Silicon Nanosheets wrapped in carbon [34]	2D	47.7%	1658	3474	~100%	1072 @ 4000	500	1297 @ 4000	1.5
Si Nanoparticle wrapped into 2D carbon Nanosheets [35]	2D	70.4%	N.A.	1723	>99%	881 @ 420	500	401 @ 3100	2.47
Porous Si with carbon wrapping [36]	3D	66.8%	N.A.	4224	>98%	1639 @ 1000	200	1074 @ 4000	N.A.
Structure-preserved 3D porous Si/reduced Graphenoxide [37]	3D	60.1%	1563	N.A.	>99%	1210 @ 500	100	955 @ 2000	0.74
Graphene encapsulated Si NPs in a CNT network [38]	3D	79%	1197	N.A.	>99%	983 @ 2000	1200	800 @ 8000	0.6

Acknowledgments

I would like to thank Prof. Graeme Blake for his supervision, guidance and suggestions for this work, even during his holidays.

References

[1] J. M. Carrasco, L. G. Franquelo, J. T. Bialasiewicz, S. Member, E. Galván, R. C. P. Guisado, S. Member, M. Ángeles, M. Prats, J. I. León, and N. Moreno-alfonso, "Power-Electronic Systems for the Grid Integration of Renewable Energy Sources : A Survey," *Ieee Transactions on Industrial Electronics*, vol. 53, no. 4, pp. 1002–1016, 2006.

[2] V. Etacheri, R. Marom, R. Elazari, G. Salitra, and D. Aurbach, "Challenges in the development of advanced li-ion batteries: a review," *Energy Environ. Sci.*, vol. 4, pp. 3243–3262, 2011.

[3] B. Fuchsbichler, C. Stangl, H. Kren, F. Uhlig, and S. Koller, "High capacity graphite-silicon composite anode material for lithium-ion batteries," *Journal of Power Sources*, vol. 196, no. 5, pp. 2889–2892, 2011.

[4] Z. L. Xu, X. Liu, Y. Luo, L. Zhou, and J. K. Kim, "Nanosilicon anodes for high performance rechargeable batteries," *Progress in Materials Science*, vol. 90, pp. 1–44, 2017.

[5] N. Nitta, F. Wu, J. T. Lee, and G. Yushin, "Li-ion battery materials: Present and future," *Materials Today*, vol. 18, no. 5, pp. 252–264, 2015.

[6] B. Sun, Z. Chen, H. S. Kim, H. Ahn, and G. Wang, "MnO/C core-shell nanorods as high capacity anode materials for lithium-ion batteries," *Journal of Power Sources*, vol. 196, no. 6, pp. 3346–3349, 2011.

[7] S. Goriparti, E. Miele, F. De Angelis, E. Di Fabrizio, R. Proietti Zaccaria, and C. Capiglia, "Review on recent progress of nanostructured anode materials for Li-ion batteries," *Journal of Power Sources*, vol. 257, pp. 421–443, 2014.

[8] C. Liu, Z. G. Neale, and G. Cao, "Understanding electrochemical potentials of cathode materials in rechargeable batteries," *Materials Today*, vol. 19, no. 2, pp. 109–123, 2016.

[9] J. Wen, Y. Yu, and C. Chen, "A Review on Lithium-Ion Batteries Safety Issues: Existing Problems and Possible Solutions," *Materials Express*, vol. 2, no. 3, pp. 197–212, 2012.

[10] A. Bordes, E. De Vito, C. Haon, A. Boulineau, A. Montani, and P. Marcus, "Multiscale Investigation of Silicon Anode Li Insertion Mechanisms by Time-of-Flight Secondary Ion Mass Spectrometer Imaging Performed on an in Situ Focused Ion Beam Cross Section," *Chemistry of Materials*, vol. 28, no. 5, pp. 1566–1573, 2016.

[11] J.-Y. Li, Q. Xu, G. Li, Y.-X. Yin, L.-J. Wan, and Y.-G. Guo, "Research progress regarding Si-based anode materials towards practical application in high energy density Li-ion batteries," *Mater. Chem. Front.*, pp. 1691–1708, 2017.

[12] N. Nitta and G. Yushin, "High-capacity anode materials for lithium-ion batteries: Choice of elements and structures for active particles," *Particle and Particle Systems Characterization*, vol. 31, no. 3, pp. 317–336, 2014.

[13] M. T. McDowell, S. W. Lee, J. T. Harris, B. A. Korgel, C. Wang, W. D. Nix, and Y. Cui, "In situ TEM of two-phase lithiation of amorphous silicon nanospheres," *Nano Letters*, vol. 13, no. 2, pp. 758–764, 2013.

[14] H. Wu and Y. Cui, "Designing nanostructured Si anodes for high energy lithium ion batteries," *Nano Today*, vol. 7, no. 5, pp. 414–429, 2012.

[15] S. W. Lee, M. T. McDowell, L. A. Berla, W. D. Nix, and Y. Cui, "Fracture of crystalline silicon nanopillars during electrochemical lithium insertion," *Proceedings of the National Academy of Sciences*, vol. 109, no. 11, pp. 4080–4085, 2012.

[16] X. H. Liu, L. Zhong, S. Huang, S. X. Mao, T. Zhu, and J. Y. Huang, "Size-dependent fracture of silicon nanoparticles during lithiation," *ACS Nano*, vol. 6, no. 2, pp. 1522–1531, 2012.

[17] P. Verma, P. Maire, and P. Novák, "A review of the features and analyses of the solid electrolyte interphase in Li-ion batteries," *Electrochimica Acta*, vol. 55, no. 22, pp. 6332–6341, 2010.

[18] A. L. Michan, G. Divitini, A. J. Pell, M. Leskes, C. Ducati, and C. P. Grey, "Solid Electrolyte Interphase Growth and Capacity Loss in Silicon Electrodes," *Journal of the American Chemical Society*, vol. 138, no. 25, pp. 7918–7931, 2016.

[19] X. H. Liu, L. Zhong, S. Huang, S. X. Mao, T. Zhu, and J. Y. Huang, "Size-dependent fracture of silicon nanoparticles during lithiation," *ACS Nano*, vol. 6, no. 2, pp. 1522–1531, 2012.

[20] X. Zuo, J. Zhu, P. Müller-Buschbaum, and Y. J. Cheng, "Silicon based lithium-ion battery anodes: A chronicle perspective review," *Nano Energy*, vol. 31, no. October 2016, pp. 113–143, 2017.

[21] I. Hasa, J. Hassoun, and S. Passerini, "Nanostructured Na-ion and Li-ion anodes for battery application: A comparative overview," *Nano Research*, vol. 10, no. 12, pp. 3942–3969, 2017.

[22] X. H. Liu, H. Zheng, L. Zhong, S. Huang, K. Karki, L. Q. Zhang, Y. Liu, A. Kushima, W. T. Liang, J. W. Wang, J. H. Cho, E. Epstein, S. A. Dayeh, S. T. Picraux, T. Zhu, J. Li, J. P. Sullivan, J. Cumings, C. Wang, S. X. Mao, Z. Z. Ye, S. Zhang, and J. Y. Huang, "Anisotropic swelling and fracture of silicon nanowires during lithiation," *Nano Letters*, vol. 11, no. 8, pp. 3312–3318, 2011.

[23] F. F. Cao, J. W. Deng, S. Xin, H. X. Ji, O. G. Schmidt, L. J. Wan, and Y. G. Guo, "Cu-Si nanocable arrays as high-rate anode materials for lithium-ion batteries," *Advanced Materials*, vol. 23, no. 38, pp. 4415–4420, 2011.

[24] X. Zhou, Y. X. Yin, L. J. Wan, and Y. G. Guo, "Self-assembled nanocomposite of silicon nanoparticles encapsulated in graphene through electrostatic attraction for lithium-ion batteries," *Advanced Energy Materials*, vol. 2, no. 9, pp. 1086–1090, 2012.

[25] N. Lin, Y. Han, L. Wang, J. Zhou, J. Zhou, Y. Zhu, and Y. Qian, "Preparation of Nanocrystalline Silicon from $SiCl_4$ at 200 °C in Molten Salt for High-Performance Anodes for Lithium Ion Batteries," *Angewandte Chemie International Edition*, pp. n/a—-n/a, 2015.

[26] J. Xie, L. Tong, L. Su, Y. Xu, L. Wang, and Y. Wang, "Core-shell yolk-shell Si @ C @ Void @ C nanohybrids as advanced lithium ion battery anodes with good electronic conductivity and corrosion resistance," *Journal of Power Sources*, vol. 342, pp. 529–536, 2017.

[27] Z. Lu, N. Liu, H. W. Lee, J. Zhao, W. Li, Y. Li, and Y. Cui, "Nonfilling carbon coating of porous silicon micrometer-sized particles for high-performance lithium battery anodes," *ACS Nano*, vol. 9, no. 3, pp. 2540–2547, 2015.

[28] J.-K. Yoo, J. Kim, H. Lee, J. Choi, M.-J. Choi, D. M. Sim, Y. S. Jung, and K. Kang, "Porous silicon nanowires for lithium rechargeable batteries," *Nanotechnology*, vol. 24, no. 42, p. 424008, 2013.

[29] I. Ryu, J. W. Choi, Y. Cui, and W. D. Nix, "Size-dependent fracture of Si nanowire battery anodes," *Journal of the Mechanics and Physics of Solids*, vol. 59, no. 9, pp. 1717–1730, 2011.

[30] B. Gattu, R. Epur, P. H. Jampani, R. Kuruba, M. K. Datta, and P. N. Kumta, "Silicon-Carbon Core-Shell Hollow Nanotubular Configuration High-Performance Lithium-Ion Anodes," *Journal of Physical Chemistry C*, vol. 121, no. 18, pp. 9662–9671, 2017.

[31] J. K. Ha, G. S. Chauhan, J. H. Ahn, H. J. Ahn, and K. K. Cho, "Electrochemical properties of enclosed silicon nanopowder electrode inserted in integrated TiO2nanotubes grown on titanium for Li-ion battery," *Electrochimica Acta*, vol. 215, pp. 674–681, 2016.

[32] D. Jia, X. Li, and J. Huang, "Bio-inspired sandwich-structured carbon/silicon/titanium-oxide nanofibers composite as an anode material for lithium-ion batteries," *Composites Part A: Applied Science and Manufacturing*, vol. 101, pp. 273–282, 2017.

[33] T. Kennedy, M. Bezuidenhout, K. Palaniappan, K. Stokes, M. Brandon, and K. M. Ryan, "Nanowire Heterostructures Comprising Germanium Stems and Silicon Branches as High-Capacity Li-Ion Anodes with Tunable Rate Capability," *ACS Nano*, vol. 9, no. 7, pp. 7456–7465, 2015.

[34] S. Chen, Z. Chen, X. Xu, C. Cao, M. Xia, and Y. Luo, "Scalable 2D Mesoporous Silicon Nanosheets for High-Performance Lithium-Ion Battery Anode," *Small*, vol. 1703361, p. 1703361, 2018.

[35] L. Yan, J. Liu, Q. Wang, M. Sun, Z. Jiang, C. Liang, F. Pan, and Z. Lin, "In Situ Wrapping Si Nanoparticles with 2D Carbon Nanosheets as High-Areal-Capacity Anode for Lithium-Ion Batteries," *ACS Applied Materials and Interfaces*, vol. 9, no. 44, pp. 38159–38164, 2017.

[36] P. Gao, H. Tang, A. Xing, and Z. Bao, "Porous silicon from the magnesiothermic reaction as a high-performance anode material for lithium ion battery applications," *Electrochimica Acta*, vol. 228, pp. 545–552, 2017.

[37] K. Zhang, Y. Xia, Z. Yang, R. Fu, C. Shen, and Z. Liu, "Structure-preserved 3D porous silicon/reduced graphene oxide materials as anodes for Li-ion batteries," *RSC Adv.*, vol. 7, no. 39, pp. 24305–24311, 2017.

[38] X. Ding, H. Wang, X. Liu, Z. Gao, Y. Huang, D. Lv, P. He, and Y. Huang, "Advanced anodes composed of graphene encapsulated nano-silicon in a carbon nanotube network," *RSC Adv.*, vol. 7, no. 26, pp. 15694–15701, 2017.

[39] "3M™ Battery Anode." `https://www.3m.com/3M/en{_}US/company-us/all-3m-products/{~}/3M-Battery-Anode/?N=5002385+3294001096{&}rt=rud`. Accessed: 2018-03-09.

[40] "XG Science INC. Si-Graphene anode." `http://xgsciences.com/products/energy-storage-materials/lithium-ion-batteries/`. Accessed: 2018-03-09.